NJC

Accepted Manuscript






ROYAL SOCIETY OF CHEMISTRY

rsc.li/njc

DOI: 10.1039/C7NJ02725G

Journal Name

ARTICLE





# Nucleophile and Base Differentiation of Pyridine in Reaction with Tetrahalocatechols and the Formation of Manganese(III)-Catecholate and Pyridinium-Catecholate Complexes for the *in situ* Generation of Hydrogen Peroxide from Dioxygen

Nicholas Bakewell[a], Rumintha Thavarajah[b], Majid Motevalli[c] and Tippu S. Sheriff*[c]

Received 00th January 20xx,
Accepted 00th January 20xx

DOI: 10.1039/x0xx00000x

www.rsc.org/

Crystal structures of two novel pyridinium catecholate compounds (1,2-dihydroxy-3,5,6-trichlorobenzene-4-pyridinium chloride and 1,2-dihydroxy-3,5,6-tribromobenzene-4-pyridinium bromide) were obtained by the reaction of pyridine with tetrachloro-*o*-benzoquinone (in the presence of hydroxylamine) and tetrabromocatechol respectively. A similar reaction with tetrachlorocatechol as a starting substrate showed pyridine to act as a base rather than a nucleophile, with a crystal structure of the pyridinium-catecholate salt obtained. The role of a number of manganese-catecholate complexes as catalysts in the reduction of dioxygen to hydrogen peroxide was also investigated. Diaqua*bis*(3,5,6-tribromobenzene-4-pyridinium catecholate)manganese(III) bromide·MeOH, [pyH][$Mn^{III}(Br_4Cat)_2(H_2O)(py)$] and [4-MepyH][$Mn^{III}(Br_4Cat)_2(H_2O)$(4-Mepy)] (where $CatH_2$ = catechol) were synthesised and characterised by melting point, FTIR, CHN (and Mn) analysis, mass spectrometry and UV-vis spectroscopy. All showed catalytic behaviour in dioxygen reduction at 20±1 °C and pH 8.00 in the presence of hydroxylamine as reducing substrate, with initial rates of hydrogen peroxide generation and turnover frequencies of up to 11.2 × $10^{-5}$ mol $dm^{-3}$ $s^{-1}$ and 8060 $hr^{-1}$ respectively in the presence of a 30-fold molar excess of ligand.

## Introduction

Hydrogen peroxide ($H_2O_2$) is a strong oxidising agent and as such, has a variety of uses in areas such as pharmaceuticals, textiles, biocides, disinfectants and bleaching.[1,2,3] As an oxidant, it is seen as a popular alternative to dioxygen ($O_2$) due to its green nature – in many cases water being the only by-product of its reduction.[4] Furthermore, the kinetic inertness of $O_2$ means $H_2O_2$ is a more suitable oxidant under ambient conditions.[5] However, the industrial process of $H_2O_2$ production via anthraquinone oxidation is a multi-step process which, aside from waste generation, requires a large amount of energy which comes at a high cost. This expense is further increased by the need for its transport and storage.[6] Thus, alternative methods for $H_2O_2$ production when not needed on

[a] graduated with an MSci in chemistry, Queen Mary University of London, 2017.
[b] graduated with a BSc in chemistry, Queen Mary University of London, 2016.
[c] Department of Chemistry and Biochemistry, Queen Mary University of London, London E1 4NS, UK. Email: t.s.sheriff@qmul.ac.uk. Tel: +44 (0) 207 882 8466.

Electronic Supplementary Information (ESI) available: ESI1 A description of ligand abbreviations. ESI2 Expanded positive mode mass spectrum showing the mass peak range of the cation (-$Br^-$) of **(3)**. ESI3 Expanded positive mode mass spectrum showing the mass peak range of the cation (-$Br^-$) of **(4)**. ESI4 Expanded negative mode peak range in the mass spectrum of the anion of complex **(6)** (with removal of the labile axial pyridine and $H_2O$ ligands). See DOI: 10.1039/x0xx00000x

View Article Online
DOI: 10.1039/C7NJ02725G




an industrial scale have been explored. One such method is the *in situ* reduction of $O_2$ to $H_2O_2$ in the presence of manganese-catecholate catalysts.[5,7,8] These complexes have been shown to catalyse this reduction in the presence of a hydroxylamine ($NH_2OH$) or hydrazine ($N_2H_4$) reducing substrate in the pH range 7.5-8.6 (eq. (1)), where $H_2Cat$ = 1,2-dihydroxybenzene (catechol) and X = $SO_3^-$, Br, Cl or other electron-withdrawing group.[9]

$$[Mn^{III}(X_mCat)_2]^{n-}$$

$$O_{2\,(g)} + 2\,NH_2OH_{\,(aq)} \rightarrow H_2O_{2\,(aq)} + 2\,H_2O_{\,(l)} + N_{2\,(g)} \qquad (1)$$

Electron deficient catechols such as tetrachlorocatechol (1,2-dihydroxy-3,4,5,6-tetrachlorobenzene, $H_2TCC$) were found to be essential ligand requirements for this system.[5] The synthesis of 1,2-dihydroxy-3,5,6-trichlorobenzene-4-pyridinium chloride **(1)** from tetrachloro-*o*-benzoquinone (TCBQ), pyridine (py) and hydroxylamine hydrochloride ($NH_2OH{\cdot}HCl$), and a crystal structure of its manganese(III) complex, chloro*bis*(3,5,6-trichlorobenzene-4-pyridinium catecholate)manganese(III) (Scheme 1), have been reported previously.[7]

of $O_2$ to $H_2O_2$.[11] Our extension of this work, reported herein, encompasses two main focal points. Firstly, an investigation into novel synthetic routes and mechanisms for the preparation of pyridinium-substituted catecholate compounds using both TCBQ and tetrabromocatechol ($H_2TBC$) as starting substrates (ESI1). Secondly, an examination of the catalytic efficacy of the related manganese(III)-catecholate complexes in the reduction of $O_2$ to $H_2O_2$ in the presence of $NH_2OH$ under ambient conditions.

## Experimental

### Materials and Equipment

$H_2TCC$ was prepared via a previously reported procedure.[12] All other reagents were purchased from Sigma-Aldrich and used without further purification. Deionised water was obtained using an Elga Purelab water purification system. Aqueous $[Ti(OH)_3(H_2O)_3]^+$ was prepared by the addition of potassium titanium oxalate (10.0 g, 28.2 mmol) to concentrated sulfuric acid (55 mL). The mixture was heated until effervescence had ceased (~30 min), cooled to room temperature and diluted to volume (500 mL) with deionised water.

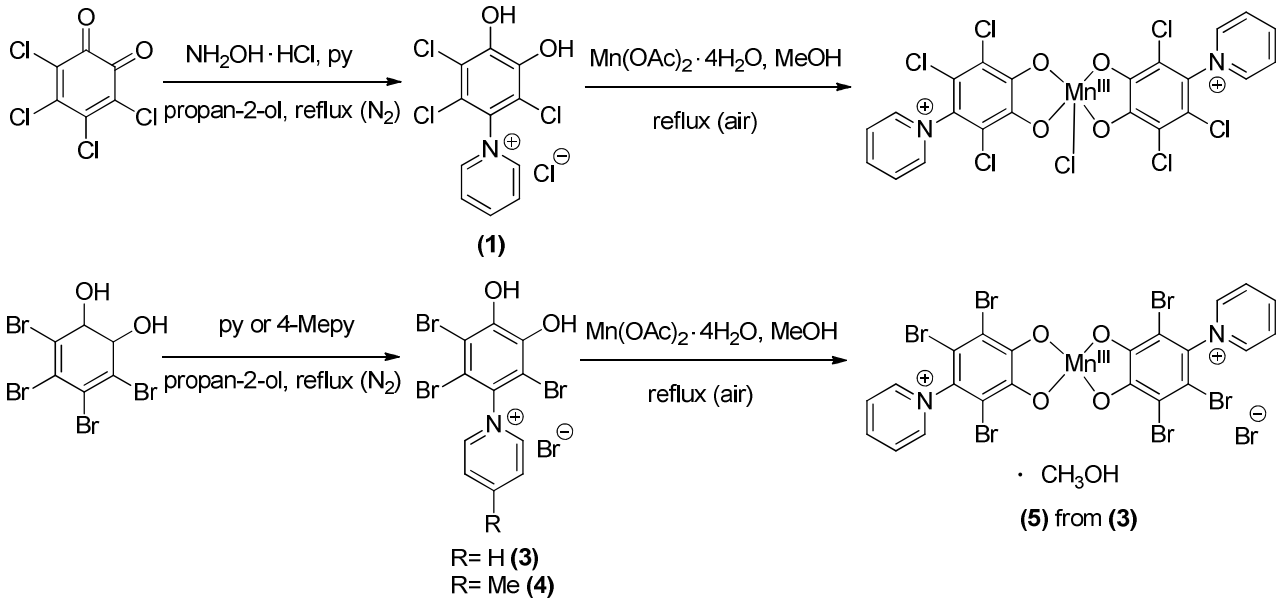


Scheme 1. *Top*: Formation of 1,2-dihydroxy-3,5,6-trichlorobenzene-4-pyridinium chloride **(1)** and subsequent preparation of chloro*bis*(3,5,6-trichlorobenzene-4-pyridinium catecholate)manganese(III).[7] *Bottom*: Formation of 1,2-dihydroxy-3,5,6-tribromobenzene-4-pyridinium bromide **(3)** 1,2-dihydroxy-3,5,6-tribromobenzene-4-(4 methylpyridinium) bromide **(4)** and diaquabis(3,5,6-tribromobenzene-4-pyridinium catecholate)manganese(III) bromide·MeOH **(5)** from **(3)**.

We also demonstrated that chloro*bis*(3,5,6-trichlorobenzene-4-pyridinium catecholate) manganese(III) was a catalyst for the formation of $H_2O_2$ via reduction of $O_2$ in the presence of $NH_2OH$ as reducing substrate.[7] One-pot syntheses of a number of manganese-catecholate complexes of a similar nature to those described above have also been reported previously.[10,11] The role of these complexes as catalysts in the oxidation of 3,5-di-*tert*-butylcatechol to 3,5-di-*tert*-butyl-1,2-benzoquinone have also been investigated with the simultaneous reduction

Aqueous $MnCl_2{\cdot}4H_2O$ was prepared by dissolving *Anala**R*** $MnCl_2{\cdot}4H_2O$ (24.7 mg, 125 µmol) in deionised water in a volumetric flask (25.0 mL). A HANNA pH meter was used to determine the pH and was calibrated periodically at pH 7 and 9. IR spectra were obtained using a PerkinElmer Spectrum 65 FT-IR spectrometer by attenuated total reflection (ATR). $^1H$ NMR spectra were recorded on a 400 MHz Bruker AVIII 400 spectrometer. The absorbance of the $[Ti(O_2)(OH)(H_2O)_3]^+$ ($Ti^{IV}$-$H_2O_2$) complex was measured at 407 nm using a Hitachi U-

View Article Online
DOI: 10.1039/C7NJ02725G
Journal Name ARTICLE



3010 UV-Vis spectrophotometer and the absorbances of prepared manganese complexes were measured using a PerkinElmer Lambda 35 UV-Vis spectrophotometer. Mass spectrometry was performed on an Agilent Technologies 1100 Series liquid chromatography-mass spectrometer or an Agilent 6890N Network GC coupled to an Agilent 5973N Mass Selective Detector (MSD). Elemental analyses for C, H and N were carried out by MEDAC Ltd, Cobham, Surrey, and Mn was determined spectrophotometrically as $MnO_4^-$ by oxidation with potassium periodate.[13] Melting points were obtained using a Gallenkamp melting point apparatus. X-ray crystal structures were collected on a Bruker Kappa Apex II Duo diffractometer with Apex II, area detector and molybdenum sealed tube x-ray sources (50 KV, 30 mA, λ=0.71073 Å). The crystal-to-detector distance was 30 mm and ϕ and Ω scans (2.0° increments, 10 s exposure time) were carried out to fill the Ewald sphere. Data collection and processing were carried out using the SAINT[14] and empirical absorption correction was applied using SADABS[15]. The structures were solved by the direct-method using the program SHELXS-2014/7[16] and refined anisotropically (non-hydrogen atoms) by full-matrix least-squares on $F^2$ using SHELXL-2014/7[17]. The H atom positions were calculated geometrically and refined with a riding model. The program SHELXTL[18] was used for drawing the molecules and for preparing the material for publication.

**Preparation of 1,2-dihydroxy-3,5,6-trichlorobenzene-4-pyridinium chloride (1)**

**From TCBQ**

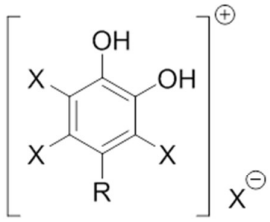

X = Cl, R = py **(1)**
X = Br, R = py **(3)**
X = Br, R = 4-Mepy **(4)**

TCBQ (0.49 g, 2.0 mmol), $NH_2OH{\cdot}HCl$ (0.16 g, 2.3 mmol) and py (0.50 mL, 6.2 mmol) were dissolved in propan-2-ol (10 mL). The solution was refluxed for 1 hr under $N_2$ with continuous stirring and slowly cooled to room temperature. A brown crystalline solid **(1)** suitable for crystallographic analysis was separated from the solution after one month (0.53 g, 81%); m.p. 226–228 °C; Found: C, 40.26; H, 2.17, N, 4.44. Calc. for $C_{11}H_7NO_2Cl_4$: C, 40.40; H, 2.16, N, 4.28 %; $\tilde{\nu}_{max}$ /cm$^{-1}$ (ATR) 3265 (O–H), 3118 (Ar C–H), 1626 (Ar C=N), 1565 (Ar C=C), 1270 (C–O), 670 (C–Cl); $\delta_H$(400 MHz; DMSO) 8.50-8.54 (2 H, t, $J_{56}$ 8, $J_{57}$ 8, py), 8.98-9.02 (1 H, t, $J_{56}$ 8, $J_{57}$ 8, py), 9.39-9.40 (2 H, d, $J_{56}$ 8, py); *m/z* (MeOH): $[M–Cl]^+$ 290.2 (expected 290.5).

**Attempted preparation from $H_2$TCC**

$H_2$TCC (0.49 g, 2.0 mmol) was dissolved in py (0.50 mL, 6.2 mmol) and propan-2-ol (10 mL). The solution was refluxed for 1 hr under $N_2$ with continuous stirring and slowly cooled to room temperature. The resulting brown solid was recrystallised from hot ethanol yielding light yellow-brown crystals **(2)** suitable for crystallographic analysis after one month (0.57 g, 88%); m.p. 86–88 °C; $\tilde{\nu}_{max}$ /cm$^{-1}$ (ATR) 3500 (free O–H), 3257 (hydrogen bonded O–H), 3071 (Ar C–H), 1613 (Ar C=N), 1533 (Ar C=C), 1262 (C–O), 668 (C–Cl).

**Preparation of 1,2-dihydroxy-3,5,6-tribromobenzene-4-pyridinium bromide (3)**

$H_2$TBC (0.85 g, 2.0 mmol) and py (0.50 mL, 6.2 mmol) were dissolved in propan-2-ol (10 mL). The solution was refluxed for 2 hr under $N_2$ with continuous stirring, forming an orange powder. Recrystallisation from hot EtOH and slow evaporation over 14 days yielded a brown crystalline solid **(3)** suitable for crystallographic analysis (0.28 g, 30%); m.p. 243–245 °C; Found: C, 26.14; H, 1.46, N, 2.74. Calc. for $C_{11}H_7NO_2Br_4$: C, 26.17; H, 1.40, N, 2.77 %; $\tilde{\nu}_{max}$ /cm$^{-1}$ (ATR) 3248 (O–H), 3124 (Ar C–H), 1625 (Ar C=N), 1571 (Ar C=C), 1278 (C–O), 671 (C–Br); $\delta_H$(400 MHz; DMSO) 7.84 (2H, s, OH), 8.49-8.53 (2H, t, $J_{56}$ 8, $J_{57}$ 8, py), 8.98-9.01 (1H, t, $J_{56}$ 8, $J_{57}$ 8, py), 9.35-9.37 (2H, d, $J_{56}$ 8, py); *m/z* (MeOH): $[M–Br]^+$ = 424.0 (expected 423.9).

**Preparation of 1,2-dihydroxy-3,5,6-tribromobenzene-4-(4-methylpyridinium) bromide (4)**

$H_2$TBC (0.85 g, 2.0 mmol) was dissolved in degassed propan-2-ol (20 mL) under $N_2$ and 4-methylpyridine (4-Mepy, 0.60 mL, 6.2 mmol) was added dropwise. The red solution was refluxed for 1 hr with stirring then left to cool slowly overnight to room temperature and further in ice yielding a red-orange solid. This was recrystallised from hot MeOH to yield a uniform red powder (4) (0.80 g, 77%), m.p. (decomposition) 204-206 °C; Found: C, 31.30; H, 1.77, N, 2.83. Calc. for $C_{12}H_9NO_2Br_4$: C, 27.78; H, 1.75, N, 2.70 %;$\bar{\nu}_{max}$/cm$^{-1}$ 3153 (O–H), 3115 and 3027 (Ar C–H), 2959 (C–H, aliphatic), 1639 (Ar C=N), 1569 (Ar C=C), 1288 (C–O), 676 (C–Br); $\delta_H$(400 MHz; DMSO) 2.75 (3 H, s, Me) 8.20-8.21 (2 H, d, $J_{56}$ 6, py), 9.05-9.07 (2 H, d, $J_{56}$ 6, py); *m/z* (DMF): $[M-Br]^+$=437.9 (expected 438.0).

**Preparation of diaqua*bis*(3,5,6-tribromobenzene-4-pyridinium catecholate)manganese(III) bromide·MeOH (5)**

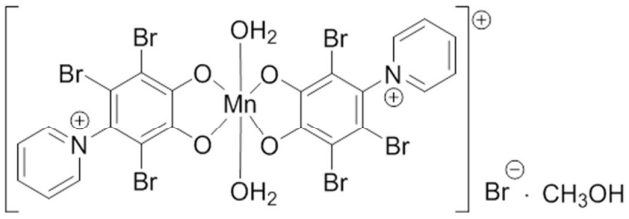

**(5)**

View Article Online
DOI: 10.1039/C7NJ02725G




1,2-dihydroxy-3,5,6-tribromobenzene-4-pyridinium bromide **(3)** (0.085 g, 0.20 mmol) and manganese(II) perchlorate hexahydrate (0.020 g, 0.080 mmol) were dissolved in MeOH (5.0 mL). $Et_3N$ (0.014 mL, 0.10 mmol) in MeOH (5.0 mL) was added dropwise over a period of 10 min. The solution was refluxed for 2 hr and cooled slowly overnight to obtain **(5)** (0.076 g, 38%) as a uniform green powdered solid; m.p. 274–276 °C; Found: C, 25.51; H, 1.72, N, 2.72. Calc. for $C_{23}H_{18}Br_7MnN_2O_7$: C, 26.34; H, 1.73, N, 2.67 %; $\tilde{\nu}_{max}$ /cm$^{-1}$ (ATR) 3122 and 3075 (Ar C–H), 1625 (Ar C=N), 1535 (Ar C=C), 1427 (C–O), 677 (C–Br); *m/z* (MeOH): $[M\text{-}Br]^+$=900.7 (expected 900.7).

**Preparation of [pyH][Mn$^{III}$(Br$_4$Cat)$_2$(H$_2$O)(py)] (6)**

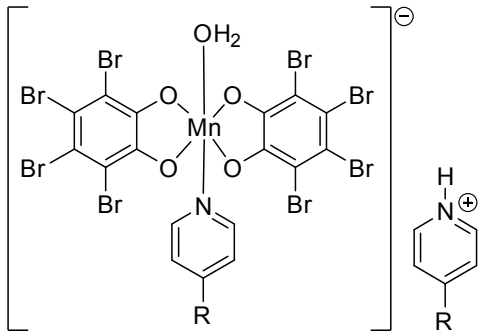


R = H **(6)**
R = Me **(7)**

Manganese(II) chloride tetrahydrate (79.0 mg, 0.399 mmol) and $H_2$TBC (0.34 g, 0.80 mmol) were dissolved in MeOH (20 mL) with stirring. Py (0.81 mL, 10 mmol) in MeOH (10 mL) was added dropwise forming an olive-green solution. This was heated to 50 °C and stirred for 30 min. The precipitate was filtered, recrystallised from hot MeOH and left to dry in air to yield a uniform dark green powder **(6)** (0.19 g, 45%), m.p. 284-288 °C; Found: C, 24.63; H, 1.25; N, 2.50; Mn, 5.32. Calc. for $C_{22}H_{13}Br_8MnN_2O_5$: C, 24.48; H, 1.21, N, 2.60; Mn, 5.09 %; $\lambda_{max}$(DMF)/nm 259 (ε/dm$^3$ mol$^{-1}$ cm$^{-1}$ 34900), 289 (21900), ~339sh (10000), 600 (163), ~682sh (140); $\bar{\nu}_{max}$/cm$^{-1}$ 3093 and 3066 (Ar C–H), 1638 and 1598 (Ar C=N), 1532 (Ar C=C), 1414 (C–O), 674 (C–Br); *m/z* (DMF): $[M\text{-}(H_2O+py)]^-$=902.1 (expected 902.3).

**Preparation of [4-MepyH][Mn$^{III}$(Br$_4$Cat)$_2$(H$_2$O)(4-Mepy)] (7)**

Manganese(II) chloride tetrahydrate (79.0 mg, 0.399 mmol) and $H_2$TBC (344 mg, 0.808 mmol) were dissolved in MeOH (20 mL) with stirring. 4-Mepy (0.97 mL, 10 mmol) in MeOH (10 mL) was added dropwise forming an olive-green solution. The solution was refluxed for 1 hr, cooled slowly to room temperature overnight and then further in ice. The precipitate was filtered, recrystallised from hot MeOH and left to dry in air yielding a uniform dark green powder **(7)** (0.38 g, 73%), m.p. 267-270 °C; Found: C, 26.13; H, 1.53; N, 2.45; Mn, 5.36. Calc. for $C_{24}H_{17}Br_8MnN_2O_5$: C, 26.03; H, 1.55; N; 2.53; Mn, 4.96 %; $\bar{\nu}_{max}$/cm$^{-1}$ 3081 and 3057 (Ar C–H), 2980 (C–H aliphatic), 1640 and 1615 (Ar C=N), 1532 (Ar C=C), 1412 (C–O), 637 (C–Br); *m/z* (DMF): $[M\text{-}(H_2O+4\text{-}Mepy)]^-$=902.1 (expected 902.3).

**Measurement of $H_2O_2$ generation**

In a typical experiment, a 100 mL solution of 1:1 ACN/deionised water containing 4-(2-hydroxyethyl)piperazine-1-propanesulfonic acid (EPPS) buffer (1.26 g, 5.00 mmol) and 50% (w/w) aqueous $NH_2OH$ solution (3.06 mL, 50.0 mmol) was adjusted to pH 8.00 with aqueous NaOH. The solution was transferred to a dreschel bottle with a sintered glass inlet and $O_2$ (0.6 L min$^{-1}$) was pumped through the solution with rapid, continuous stirring (1500 rpm) while maintained at 20±1 °C. After the addition of diaqua*bis*(3,5,6-tribromobenzene-4-pyridinium catecholate)manganese(III) bromide·MeOH **(5)** (0.0049 g, 5.0 μmol), 0.100 mL aliquots of reaction solution were transferred to $[Ti(OH)_3(H_2O)_3]^+$ solution (2.00 mL) at regular time intervals. The formation of the yellow-coloured $[Ti(O_2)(OH)(H_2O)_3]^+$ complex with a $\lambda_{max}$ of 407 nm (ε = 770 dm$^3$ mol$^{-1}$ cm$^{-1}$) allowed quantification of $[H_2O_2]$ at each time interval. This experiment was repeated with the addition of a 30-fold molar excess of **(3)**. Experiments were also carried out with $H_2$TBC (1.50 mM, 30-fold molar excess over Mn) and either **(6)** (0.0054 g, 5.0 μmol) or **(7)** (0.0055 g, 5.0 μmol) instead of **(5)**. In addition a similar procedure was followed with the exception of the addition of aqueous $MnCl_2.4H_2O$ (1.00 mL, 5.00 mM) and desired ligand ($H_2$TBC or compound **(3)** in either 2-fold or 30-fold molar excess over Mn) to the starting solution that allowed *in situ* formation of the complex.

## Results and Discussion

**Crystal structures of (1), (2) and (3) and proposed mechanisms**

The reflux of TCBQ with $NH_2OH$·HCl and py in propan-2-ol under $N_2$ led to the formation of 1,2-dihydroxy-3,5,6-trichlorobenzene-4-pyridinium chloride **(1)** as a brown crystalline solid in an 81% yield with a sharp melting point of 226-228 °C. The expected hydrogen environments were present in the $^1$H NMR spectrum. A crystal structure for **(1)** was acquired and was as expected with the addition of a molecule of propan-2-ol which stabilises the structure through hydrogen bonding (Fig. 1).

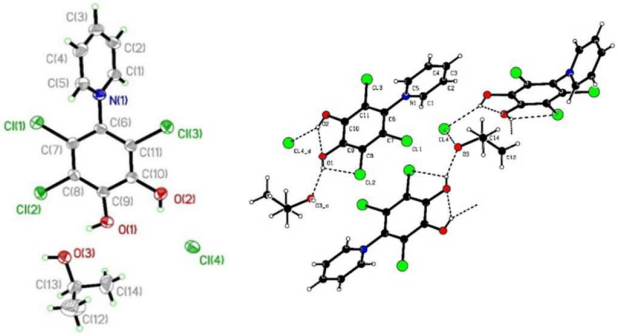


**Fig. 1.** X-ray crystal structure of 1,2-dihydroxy-3,5,6-trichlorobenzene-4-pyridinium chloride **(1)** (*left*) and crystal structure of **(1)** showing the hydrogen bonding interactions (*right*).

View Article Online
DOI: 10.1039/C7NJ02725G





The structure of **(1)** comprises a planar chlorocatechol ring with a planar pyridinium substituent attached in the 4-position. These rings are non-coplanar which may allow for more favourable electrostatic interactions between proximal chlorine atoms on the catechol and hydrogen atoms on the pyridinium substituent. The positioning of the chloride ion is presumably to maximise electrostatic interactions with the protic hydrogens of the –OH groups leading to increased stabilisation. Selected bond lengths and bond angles for 1,2-dihydroxy-3,5,6-trichlorobenzene-4-pyridinium chloride **(1)** are provided in Table 1.

| Bond lengths /Å | | Bond angles /° | |
|---|---|---|---|
| C1–N1 | 1.346(3) | N1–C1–C2 | 119.8(2) |
| C1–H1A | 0.93 | N1–C1–H1A | 120.1 |
| C1–C2 | 1.366(3) | C1–C2–C3 | 119.7(2) |
| C6–C11 | 1.394(3) | C7–C6–N1 | 119.68(19) |
| C6–N1 | 1.449(3) | C6–C7–Cl1 | 120.20(17) |
| C10–O2 | 1.352(3) | C9–C8–C7 | 120.6(2) |
| C11–C13 | 1.726(2) | C1–N1–C6 | 119.61(18) |
| O1–H1 | 0.88 | C9–O1–H1 | 109.5 |

**Table 1.** Selected bond lengths (Å) and angles (◦) for **(1)**.

We proposed two possible pathways for this reaction. In the first pathway, TCBQ is reduced by $NH_2OH$ forming $H_2TCC$, followed by the nucleophilic aromatic substitution of chlorine at the 4-position by py, resulting in the elimination of the chloride ion. Alternatively, if reduction by $NH_2OH$ occurs after substitution, the mechanism can be explained via a Michael addition of py and elimination of chloride, followed by reduction to form the substituted catechol (Scheme 2).

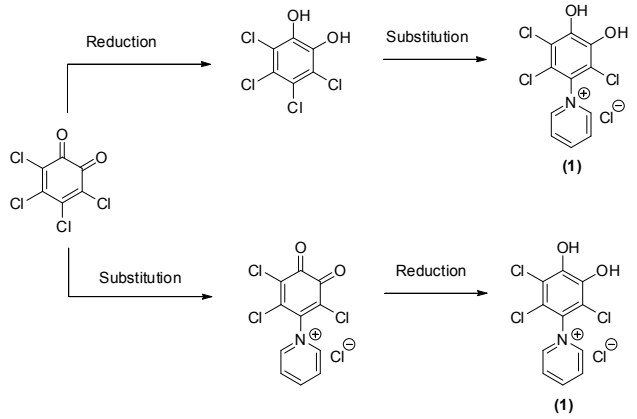


**Scheme 2.** Possible pathways for the preparation of **(1)** from TCBQ.

Reflux of $H_2TCC$ with py in propan-2-ol under $N_2$ did not yield the expected product **(1)**. A crystal structure of the product obtained **(2)** consisted of a pyridinium ion ($pyH^+$) hydrogen bonded to $HTCC^-$, which is mono-deprotonated at the 2-position (Fig. 2).

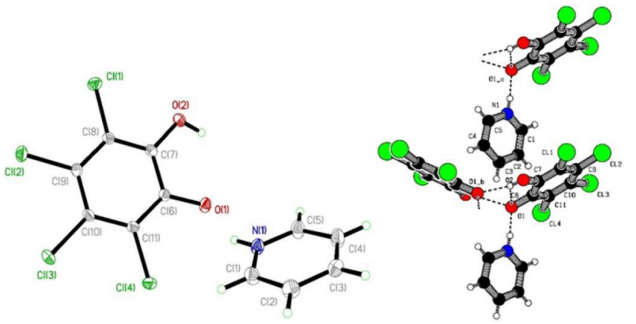

**Fig. 2.** (X-ray crystal structure of **(2)** (*left*) and crystal structure showing the hydrogen bonding in **(2)** (*right*).

The isolation of this pyridinium catecholate salt, [$pyH^+$][$HTCC^-$], as a crystal structure is unusual and is interesting in the context of this work as it shows pyridine acting as both a base and a nucleophile. Selected bond lengths and bond angles for the obtained crystal structure **(2)** are provided in Table 2.

| Bond lengths /Å | | Bond angles /° | |
|---|---|---|---|
| C1–N1 | 1.3398(15) | N1–C1–C2 | 121.53(10) |
| C1–C2 | 1.3939(16) | N1–C1–H1 | 119.2 |
| C1–H1 | 0.95 | C3–C2–C1 | 118.76(10) |
| C5–N1 | 1.3417(14) | C3–C2–H2 | 120.6 |
| C6–O1 | 1.3392(12) | O1–C6–C11 | 123.70(9) |
| C6–C11 | 1.4015(15) | O1–C6–C7 | 118.07(8) |
| C6–C7 | 1.4148(18) | C11–C6–C7 | 118.22(9) |
| C7–O2 | 1.3547(14) | C10–C9–Cl2 | 120.42(7) |
| C8–Cl1 | 1.7218(18) | C6–C11–C10 | 122.00(9) |
| C9–Cl2 | 1.7280(12) | C6–C11–Cl4 | 117.74(8) |
| N1–H1A | 0.88 | C1–N1–C5 | 120.05(10) |
| O1–H1A | 1.697 | C1–N1–H1A | 120.0 |
| O1–H2A | 2.307 | C7–O2–H2A | 109.5 |
| O2–H2A | 0.84 | | |

**Table 2.** Selected bond lengths (Å) and angles (°) for **(2)**.

These results indicate that instead of acting as a nucleophile, substituting the chlorine atom in the 4-position of the $H_2TCC$, py acts as a base under these conditions, deprotonating one of the catechol –OH groups. The crystal structure of **(2)** shows that the deprotonated hydroxyl group of the catechol ring is hydrogen bonded not only to the pyridinium cation (O1···H1A = 1.697 Å), but also to the adjacent –OH group on the catechol ring O1···H2A = 2.307 Å) to provide maximum stabilisation. The fact that nucleophilic aromatic substitution using py did not occur on $H_2TCC$ suggests when using TCBQ as a starting material, the second suggested pathway (Scheme 2) is followed, with nucleophilic substitution first, followed by reduction to the catechol product. With this result in mind, we investigated the behaviour of py when using $H_2TBC$ as the substrate. Interestingly, reflux of the readily available $H_2TBC$ with py in propan-2-ol under $N_2$, followed by recrystallisation from EtOH led to the formation of 1,2-dihydroxy-3,5,6-tribromobenzene-4-pyridinium bromide **(3)** in a 30% yield as a brown crystalline solid with a sharp melting point of 243-245 °C. There is only one other reference to the preparation of **(3)**

View Article Online
DOI: 10.1039/C7NJ02725G




in the literature and involves mixing $H_2$TBC with dry py at room temperature.[19] The yellow needles obtained were characterised by elemental analysis as the pyridine adduct *viz.* **(3)**·py that had a melting point of 155-157 °C (decomp.); when the py used contained 2-3% $H_2O$, a dipyridine salt consisting of red needles which turn yellow at about 120 °C was first formed. The positive mode mass spectrum of **(3)** found in this work was as expected for the 1,2-dihydroxy-3,5,6-tribromobenzene-4-pyridinium cation (ESI2), and the expected hydrogen environments were also present in the $^1$H NMR spectrum. A crystal structure of **(3)** was obtained with the unit cell containing an additional molecule of EtOH as well as the expected product. Within the unit cell a negatively charged bromide ion is stabilised by hydrogen bonding to one of the catecholate –OH groups and an EtOH molecule (Fig. 3).

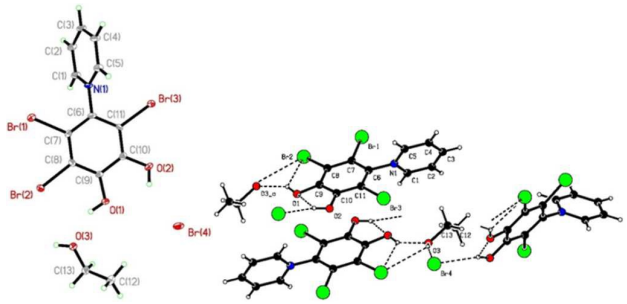

**Fig. 3.** X-ray crystal structure of 1,2-dihydroxy-3,5,6-tribromobenzene-4-pyridinium bromide **(3)** (*left*) and crystal structure of **(3)** showing the hydrogen bonding (*right*).

Typical bond lengths and bond angles for the obtained crystal structure of **(3)** are provided in Table 3.

| Bond lengths /Å | | Bond angles /o | |
|---|---|---|---|
| C1–N1 | 1.351(3) | N1–C1–C2 | 119.4(2) |
| C5–H5 | 0.95 | N1–C1–H1 | 120.3 |
| C1–C2 | 1.366(3) | C1–C2–C3 | 119.2(2) |
| C6–C11 | 1.387(3) | C7–C6–N1 | 120.4(2) |
| C6–N1 | 1.430(3) | C6–C7–Br1 | 120.12(17) |
| C10–O2 | 1.341(3) | C7–C8–C9 | 120.6(2) |
| Br1–C7 | 1.871(2) | C1–N1–C6 | 118.0(2) |
| O1–H1A | 0.84 | C9–O1–H1A | 109.5 |

**Table 3.** Selected bond lengths (Å) and angles (°) for **(3)**.

The crystal structure of **(3)** is analogous to that of **(1)** in terms of the non-coplanarity of the bromocatechol ring and its pyridinium substituent, as well as the proximity of the bromide ion to the catechol –OH groups, all of which presumably allow for optimised electrostatic stabilisation. $NH_2OH$·HCl is not required for this reaction as the $H_2$TBC starting material is already in the catechol form. This reaction can consequently be described as a nucleophilic aromatic substitution leading to the formation of compound **(3)**. It is apparent that nucleophilic aromatic substitution on catechols by py may be dependent on the nature of the substituents on the catechol. The stronger electron-withdrawing effects of the chlorine substituents on $H_2$TCC may increase the ability of the –OH groups to become deprotonated and occurs preferentially over substitution. Conversely, the lower electron-withdrawing effect of the bromine atoms in $H_2$TBC favours nucleophilic aromatic substitution. Reflux of $H_2$TBC and 4-Mepy in propan-2-ol under $N_2$ gave **(4)** as a red powder with a yield of 77%. The compound decomposed at 204-206 °C. Recrystallisation was not possible due to the product's poor solubility in all solvents tested and therefore no crystal structure was obtained. However, various analytical techniques were used to support the successful formation of the product with a high degree of confidence. The positive mode mass spectrum of **(4)** was as expected for the 1,2-dihydroxy-3,5,6-tribromobenzene-4-(4-methylpyridinium) cation (ESI3) and the expected hydrogen environments were also present in the $^1$H NMR spectrum.

Based on the results obtained, a suggested mechanism for nucleophilic substitution with TCBQ as a starting material is shown in Scheme 3.

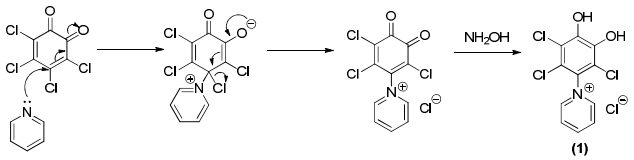

Scheme 3. Proposed mechanism for the synthesis of **(1)** from TCBQ and py via Michael addition-elimination, followed by reduction.

In contrast to $H_2$TCC, when using $H_2$TBC as a starting material, nucleophilic aromatic substitution is successful. One possible mechanism involves an addition-elimination whereby the nucleophile attacks the *para* carbon, with stabilisation of the negative charge in the intermediate, followed by the elimination of the bromine (Scheme 4).

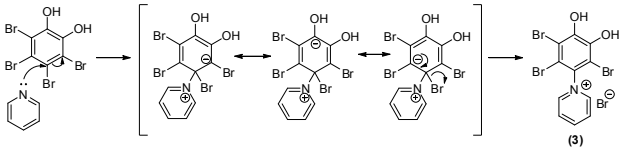

Scheme 4. A proposed mechanism for the nucleophilic aromatic substitution of the p-bromine of $H_2$TBC with py via addition-elimination.

However, the presence of the *ipso*-hydroxyl group provides some doubt to this mechanism due to its mesomeric electron-donating character. The role of py as a base, as in the synthesis of **(2)**, can be used to support a second possible mechanism for this reaction whereby deprotonation of the *ipso*-hydroxyl group initiates the departure of the bromine at the 4-position, with subsequent attack of the carbene by the py nucleophile (Scheme 5), for which there is some literature precedent.[20, 21]

View Article Online
DOI: 10.1039/C7NJ02725G





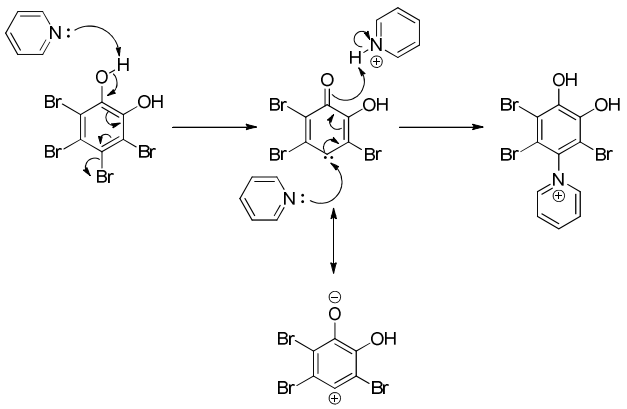

Scheme 5. A proposed mechanism for nucleophilic aromatic substitution of the *p*-bromine of $H_2$TBC by py via elimination-addition.

The observed difference in behaviour of $H_2$TCC and $H_2$TBC toward pyridine is interesting and requires further investigation. Given that the predicted pKa of $H_2$TCC and $H_2$TBC are quite similar (5.68±0.33 and 5.50±0.33 respectively)[22], it is possible that because –Br is a better leaving group than –Cl this tips the balance in favour nucleophilic aromatic substitution of $H_2$TBC.

**Formation of manganese complexes (5), (6) and (7)**

The reaction of 1,2-dihydroxy-3,5,6-tribromobenzene-4-pyridinium bromide **(3)** with manganese(II) perchlorate hexahydrate and $Et_3N$ in MeOH was carried out under reflux for 2 hr. During the reflux, a colour change from orange to green was observed, which suggested the formation of a manganese(III)-catecholate complex.[9] A green powder, **(5)**, was isolated. The previously reported analogous reaction with 1,2-dihydroxy-3,5,6-trichlorobenzene-4-pyridinium chloride **(1)** produced chloro*bis*(3,5,6-trichlorobenzene-4-pyridiniumcatecholate)manganese(III).[7] It was therefore expected that using **(3)** as a starting material would lead to the formation of bromo*bis*(3,5,6-tribromobenzene-4-pyridiniumcatecholate)manganese(III). However, the mass spectrum *m/z*: $[M\text{-}Br]^+$ peak at 900.7 did not correspond to the expected value of 980.59. This suggested that the bromide ion did not coordinate to the manganese(III) centre in complex **(5)** but rather acted as a counterion to the complex cation. This may be because the bromide ion is too large to fit within the coordination sphere of the manganese(III) centre, which in any case will be weakened due to the Jahn-Teller distortion in a manganese(III) $d^4$ octahedral or square pyramidal system. Presumably it is more energetically favourable for the bromine atom to be outside the coordination sphere. C, H and N elemental analysis indicated the presence of one molecule of MeOH and two molecules of $H_2O$ for each molecule of the manganese(III) complex, with a possibility of the two $H_2O$ molecules being situated within the coordination sphere as axial ligands. The sharp melting point of 274-276 °C suggested that the product was pure. The presence of a broad O–H peak at 3410 $cm^{-1}$ and C–H aliphatic stretch at 2950 $cm^{-1}$ suggests the presence of MeOH and possibly $H_2O$ in the compound which provides further evidence for the assigned formula from the C, H and N elemental analysis. An attempt to produce $[pyH][Mn^{III}(Br_4Cat)(Br_3pyCat)(py)_2]$ with one of the catechol ligands being *p*-substituted with py was carried out following a previously reported method.[10] A solution of manganese(II) chloride tetrahydrate, $H_2$TBC, and a large excess of py in methanol was heated to 50 °C and stirred for 30 min. It was reported that subsequent cooling to room temperature would lead to the formation of dark green crystals of $[Mn^{III}(Br_4Cat)(Br_3pyCat)(py)_2]$. However, the product precipitated from the hot solution and only a green powder was isolated. Furthermore, analysis of the product indicated no nucleophilic aromatic substitution had occurred. In fact, the isolated product was found to be $[pyH][Mn^{III}(Br_4Cat)_2(H_2O)(py)]$ **(6)**. The negative mode mass spectrum displayed a group of peaks (max. peak = 902.1) which coincides with the presence of the $[Mn^{III}(Br_4Cat)_2]^-$ anion (ESI4). C, H, N and Mn elemental analysis suggested that as well as the $pyH^+$ counterion, a py molecule and an $H_2O$ molecule were also present in the complex. These could be present as axial ligands leading to coordinative saturation of the manganese(III) centre. The lability of these ligands can be used to explain why they are not present in the mass spectrum. The presence of the py in the product was confirmed with the bifurcated peaks at 1637 $cm^{-1}$ and 1598 $cm^{-1}$. These peaks are characteristic of pyridyl C=N stretching and are present at different wavenumbers for $[Mn^{III}(Br_4Cat)(Br_3pyCat)(py)_2]$ (1622 and 1592 $cm^{-1}$).[10] The appearance of two bands also indicates there are two distinctive py-based environments within the structure, which can be assigned to coordinated py and the $pyH^+$ counterion. To attempt to prepare $[4\text{-}MepyH][Mn^{III}(Br_4Cat)(Br_3(4\text{-}Mepy)Cat)(4\text{-}Mepy)_2]$, a solution of manganese(II) chloride tetrahydrate, $H_2$TBC and 4-Mepy was refluxed in MeOH. As for **(6)**, the product precipitated from the hot solution as a dark green powder. The isolated product showed again that no nucleophilic aromatic substitution had occurred and subsequent analysis identified the product as $[4\text{-}MepyH][Mn^{III}(Br_4Cat)_2(H_2O)(4\text{-}Mepy)]$ **(7)**. This is analogous to **(6)** but with 4-Mepy replacing py in the final compound. The negative mode mass spectrum displayed the same group of peaks as for **(6)**, corresponding to the $[Mn^{III}(Br_4Cat)_2]^-$ anion. C, H, N and Mn elemental analysis suggested the presence of one 4-Mepy and one $H_2O$ molecule with peaks at 1615 $cm^{-1}$ and 1641 $cm^{-1}$ in the IR spectrum indicating the presence of two distinct pyridyl environments (one 4-Mepy axially coordinated and one $4\text{-}MepyH^+$ counterion).

**$H_2O_2$ generation studies**

Using the pre-prepared complex **(5)** as catalyst, we measured the concentration of $H_2O_2$ generated from $O_2$ in the presence of $NH_2OH$ as reducing substrate under ambient conditions (Fig. 4).

View Article Online
DOI: 10.1039/C7NJ02725G




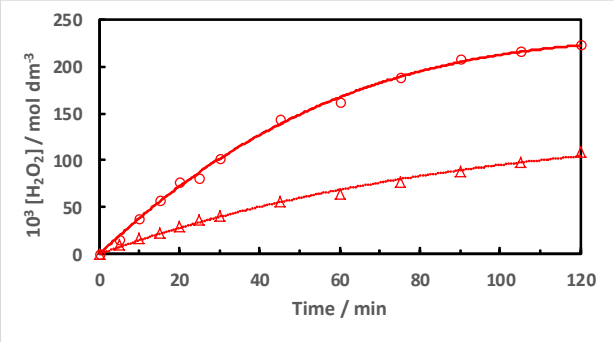


**Fig. 4.** The catalytic reduction of $O_2$ to $H_2O_2$ at 20±1 °C in a 1:1 aqueous acetonitrile solution (100 mL) at pH 8.00 with either: (○) complex **(5)** (0.050 mM) and **(3)** (1.50 mM) or (Δ) complex **(5)** (0.050 mM) only. The initial [$NH_2OH$] was 0.500 M, [EPPS] was 50.0 mM, and $O_2$ (0.6 L $min^{-1}$) was bubbled through the rapidly stirred (1500 rpm) solution. Each curve is taken as an average of two consecutive runs.

The mean initial rate of $H_2O_2$ production was calculated as 2.40 × $10^{-5}$ mol $dm^{-3}$ $s^{-1}$ with a mean turnover frequency (TOF = moles of $H_2O_2$ generated per mole of catalyst per hour) of 1730 $hr^{-1}$. We also repeated this experiment but with addition of a 30-fold excess of ligand **(3)** which increased catalytic efficacy, giving an initial rate of $H_2O_2$ production of 6.88 × $10^{-5}$ mol $dm^{-3}$ $s^{-1}$ with a TOF of 4950 $hr^{-1}$. Under the same conditions but in the absence of added catalyst, no $H_2O_2$ could be detected in the solution. Earlier work has also shown that in the absence of catechol ligand (but with $Mn^{II}$ added) negligible amounts of $H_2O_2$ are produced and that very little catalytic activity was observed with other 1st row TM *e.g.* $Cu^{II}$, $Fe^{II}$ and $Co^{II}$ in this 'enzyme-like' system.[5] We then investigated how the catalytic efficacy would be affected by generating the catalyst *in situ* rather than adding the previously isolated catalyst **(5)**. An identical procedure was followed, with the exception of the addition of aqueous manganese(II) chloride (0.050 mM) instead of complex **(5)** and a 2-fold or 30-fold (Fig. 5) molar equivalent of ligand **(3)** with respect to the moles of manganese.

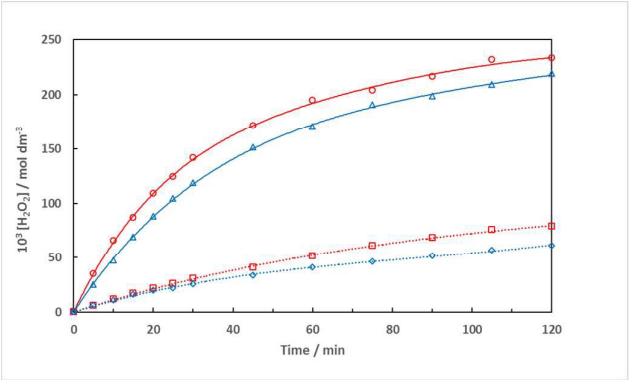


**Fig. 5.** The catalytic reduction of $O_2$ to $H_2O_2$ at 20±1 °C in a 1:1 aqueous acetonitrile solution (100 mL) at pH 8.00 with either: (○) aqueous $MnCl_2{\cdot}4H_2O$ (0.050 mM) and $H_2TBC$ (1.50 mM); (Δ) aqueous $MnCl_2{\cdot}4H_2O$ (0.050 mM) and **(3)** (1.50 mM); (□) aqueous $MnCl_2{\cdot}4H_2O$ (0.050 mM) and $H_2TBC$ (0.10 mM); or (◊) aqueous $MnCl_2{\cdot}4H_2O$ (0.050 mM) and **(3)** (0.10 mM). The initial [$NH_2OH$] was 0.500 M, [EPPS] was 50.0 mM, and $O_2$ (0.6 L $min^{-1}$) was bubbled through the rapidly stirred (1500 rpm) solution. Each curve is taken as an average of two consecutive runs.

The mean initial rates of $H_2O_2$ production were calculated to be 1.86 × $10^{-5}$mol $dm^{-3}$ $s^{-1}$ and 7.99 × $10^{-5}$ mol $dm^{-3}$ $s^{-1}$ for a 2-fold and 30-fold molar equivalent of ligand respectively, with TOFs of 1340 $hr^{-1}$ and 5740 $hr^{-1}$ respectively. With a 30-fold equivalent of $H_2TBC$ the yield of $H_2O_2$ (~0.24 mol $dm^{-3}$) is >95% based on $NH_2OH$ (eq. (1)). From these results it can be seen that the catalytic reduction of $O_2$ to $H_2O_2$ can be performed with similar efficacy whether the catalyst is pre-prepared or created *in situ*. These results also agree with past research which indicated that a higher molar excess of ligand leads to an improved rate of $H_2O_2$ generation.[9] With an excess of ligand in solution, it is conceivable that a *tris*-manganese-catecholate complex may be formed which could lead to increased catalytic activity. It has been suggested that the Jahn-Teller distortion experienced by octahedral manganese(III) complexes makes formation of a *tris*-manganese(III)-catecholate complex unfavourable due to the short "bite distance" of the catechol ligands[23], though this has since been disproved.[24] Furthermore, in the presence of excess $NH_2OH$, reduction of the manganese(III) centre to manganese(II) would remove this distortion and could increase the possibility of a *tris*-manganese(II)-catecholate complex being formed *in situ*. Further investigation into the mechanism of this catalytic reaction is necessary as it is not certain whether vacant sites at the manganese centre are needed for $O_2$ reduction. We also investigated how the presence of the pyridinium substituent on the catechol ligand affects the performance of the catalyst. To do so, we again prepared the manganese-catecholate complex *in situ* but using a 2-fold and 30-fold molar excess of $H_2TBC$ (Fig. 5). It has been shown previously that increasing the number of chlorine atoms on the catechol ligand increases initial rates of $H_2O_2$ generation, as well as TOFs.[5] It would be expected therefore, that substitution of the *p*-bromine on $H_2TBC$ for a positively charged, more strongly electron-withdrawing py would result in an increase in initial rate of $H_2O_2$ production. However, the opposite effect was observed. Initial rates for $H_2TBC$ were higher than those for compound **(3)** at 1.92 × $10^{-5}$ mol $dm^{-3}$ $s^{-1}$ and 11.1 × $10^{-5}$ mol $dm^{-3}$ $s^{-1}$ for a 2-fold and 30-fold equivalent of ligand respectively, with TOFs of 1380 $hr^{-1}$ and 8000 $hr^{-1}$ respectively. It appears that the presence of the pyridine ring deactivates the catalyst and lowers its performance. This would suggest that there is a threshold within which electron-withdrawing substituents on catechol ligands aid the reduction of $O_2$ to $H_2O_2$. Beyond this threshold, increasing electron-withdrawal leads to a decrease in catalytic efficacy. This effect has been reported previously where the presence of very strongly electron-withdrawing – $NO_2$ substituents on the catechol ring resulted in a decrease in catalytic efficacy.[5] Finally, we investigated the behaviour of complexes **(6)** and **(7)** as catalysts in this reaction in the presence of a 30-fold molar equivalent of $H_2TBC$ (Fig. 6).

View Article Online
DOI: 10.1039/C7NJ02725G





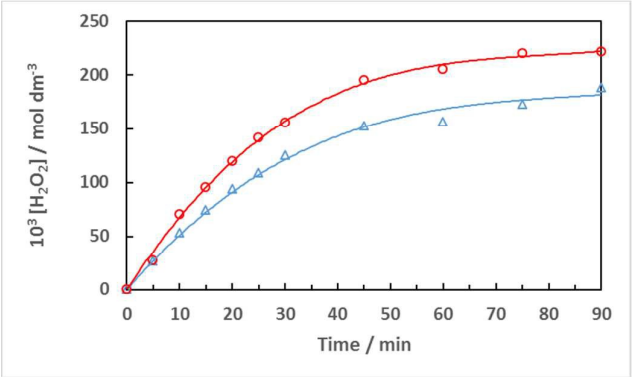


**Fig. 6.** The catalytic reduction of $O_2$ to $H_2O_2$ at 20±1.0 °C in a 1:1 aqueous acetonitrile solution (100 mL) at pH 8.00 with $H_2$TBC (1.50 mM) and either (○) complex **(7)** (0.050 mM) or (Δ) complex **(6)** (0.050 mM). The initial [$NH_2OH$] was 0.500 M, [EPPS] was 50.0 mM, and $O_2$ (0.6 L $min^{-1}$) was bubbled through the rapidly stirred (1500 rpm) solution. Each curve is taken as an average of two consecutive runs.

Both complexes **(6)** and **(7)** showed catalytic behaviour in the reduction of $O_2$ to $H_2O_2$ in the presence of $NH_2OH$, with initial rates of $H_2O_2$ generation of 8.88 × $10^{-5}$ mol $dm^{-3}$ $s^{-1}$ and 11.2 × $10^{-5}$ mol $dm^{-3}$ $s^{-1}$ respectively and TOFs of 6390 $hr^{-1}$ and 8060 $hr^{-1}$ respectively. The additional methyl group on the axial py ligand in **(7)** would be expected to increase electron density on the manganese centre in comparison to **(6)**. The results show that this improves catalytic efficacy in the generation of $H_2O_2$. It has been shown previously that the catalytic efficacy of the manganese-catecholate complexes in this system is very sensitive to the electron density on the metal centre, with what appears to be an optimum electron density for maximum efficacy. The best catalytic results obtained here are somewhat similar, but perhaps lower, to those reported previously for $[Na]_5[Mn(3,5\text{-}(SO_3)_2Cat)_2]\cdot 10H_2O$ in aqueous solution with a TOF of ~10,000 $hr^{-1}$ with a 30-fold molar excess of the ligand (Table 4).[9]

**Table 4.** Initial rates and TOFs for various catalyst and ligand systems in this and previous work.

| Fig. | Catalyst/ 0.050 mM | Ligand | Ligand/ Catalyst ratio | $10^5$ Initial Rate / mol $dm^{-3}$ $s^{-1}$ (TOF/ $hr^{-1}$) | Ref. |
|---|---|---|---|---|---|
| 4 | **(5)** | **(3)** | 2 | 2.40 (1730) | † |
| 4 | **(5)** | **(3)** | 30 | 6.88 (4950) | † |
| 5 | Aq. $MnCl_2{\cdot}4H_2O$ | $H_2$TBC | 30 | 11.1 (8000) | † |
| 5 | Aq. $MnCl_2{\cdot}4H_2O$ | **(3)** | 30 | 7.99 (5740) | † |
| 5 | Aq. $MnCl_2{\cdot}4H_2O$ | $H_2$TBC | 2 | 1.92 (1380) | † |
| 5 | Aq. $MnCl_2{\cdot}4H_2O$ | **(3)** | 2 | 1.86 (1340) | † |
| 6 | **(7)** | $H_2$TBC | 30 | 11.2 (8060) | † |
| 6 | **(6)** | $H_2$TBC | 30 | 8.88 (6390) | † |
| | $[Na]_5[Mn(3,5\text{-}(SO_3)_2Cat)_2]\cdot 10H_2O$ | 3,5-$(SO_3)_2H_2$Cat | 30 | 14.4 (10400)^ | 9 |
| | $[Na]_5[Mn(3,5\text{-}(SO_3)_2Cat)_2]\cdot 10H_2O$ | 3,5-$(SO_3)_2H_2$Cat | 2 | 1.48 (1070)^ | 9 |

TOF: turnover frequency (moles of $H_2O_2$ per mole of catalyst per hour). ^ in aq. soln. † This work.

This therefore supports the sensitivity of the catalytic system to the electronic effect of the substituents on the catechol ring and that fine tuning this 'enzyme-like' system is possible.

## Conclusions

We have successfully demonstrated new synthetic routes to pyridinium-substituted halogenocatechols using both TCBQ and $H_2$TBC as starting substrates. Crystal structures have been obtained for 1,2-dihydroxy-3,5,6-trichlorobenzene-4-pyridinium chloride **(1)** and 1,2-dihydroxy-3,5,6-tribromobenzene-4-pyridinium bromide **(3)**. A crystal structure of an unexpected pyridinium salt of a mono-deprotonated $H_2$TCC was also obtained indicating that py can function as either a nucleophile or a base, depending on the nature of the catechol starting substrate. This differentiation of py in acting as a base or a nucleophile within very similar starting substrates is interesting and merits further investigation, including theoretical studies. We also prepared diaqua*bis*(3,5,6-tribromobenzene-4-pyridiniumcatecholate)manganese(III) bromide·MeOH **(5)** from catechol **(3)**, which performed as a catalyst in the reduction of $O_2$ to $H_2O_2$ using $NH_2OH$ as reducing substrate with an initial rate of $H_2O_2$ generation of 2.40 × $10^{-5}$ mol $dm^{-3}$ $s^{-1}$ and TOF of 1730 $hr^{-1}$. The use of this catalyst with addition of a 30-fold equivalent of ligand **(3)** showed an increase in catalytic efficacy, with initial rate of 6.88 × $10^{-5}$ mol $dm^{-3}$ $s^{-1}$ and TOF of 4950 $hr^{-1}$. Furthermore, preparing the catalyst *in situ* using a 30-fold molar equivalent of $H_2$TBC instead of **(3)** led to even greater catalytic performance with initial rate of 11.1 × $10^{-5}$ mol $dm^{-3}$ $s^{-1}$ and TOF of 8000 $hr^{-1}$, indicating that presence of the pyridinium substituent appears to deactivate the catalyst and hinder its performance. Finally, we prepared two similar catalysts in $[pyH][Mn^{III}(Br_4Cat)_2(H_2O)(py)]$ **(6)** and $[4\text{-MepyH}][Mn^{III}(Br_4Cat)_2(H_2O)(4\text{-Mepy})]$ **(7)**. Complex **(7)**, with a 30-fold molar equivalent of $H_2$TBC, exhibited an initial rate and TOF that was the highest observed in this work and significantly higher than **(6)** under the same conditions. This shows the subtle electronic effect of the 4-Me group in this 'enzyme-like' system.

## Acknowledgements

The authors would like to thank Dr I. Abrahams for helping to respond to reviewers comments on the crystal structures of **(2)** and **(3)** and Dr P. B. Wyatt, also in the Department of Chemistry and Biochemistry at Queen Mary University of London, for helpful discussions on the mechanism for nucleophilic aromatic substitution and the provision of references to support the mechanism proposed in Scheme 5. We would also like to thank Dr Lingzhi Gong in Analytical Services in the Department for his help in running mass spectra.

## Notes and References

‡The crystal structures have been deposited at the Cambridge Crystallographic Data Centre with the following CCDC reference numbers: **(1)** 1564273; **(2)** 1564275; **(3)** 1564274.

1 W. Chen, S. Cai, Q.-Q. Ren, W. Wen and Y.-D. Zhao, *Analyst*, 2012, **137**, 49.
2 E. Linley, S. P. Denyer, G. McDonnell, C. Simons and J. Y. Maillard, *J. Antimicrob. Chemother.*, 2012, **67**, 1589.
3 D. Veghini, M. Bosch, F. Fischer and C. Falco, *Catal. Commun.*, 2008, **10**, 347.

View Article Online
DOI: 10.1039/C7NJ02725G


4 C. L. Hill, in *Catalytic Oxidations with Hydrogen Peroxide as Oxidant*, ed. G. Strukel, Kluwer, Dordrecht, 1992, p. 256.
5 T. S. Sheriff, *J. Chem. Soc. Dalton Trans.*, 1992, 1051.
6 J. M. Campos-Martin, G. Blanco-Brieva and J. L. G. Fierro, *Angew. Chem. Int. Ed.*, 2006, **45**, 6962.
7 T. S. Sheriff, M. Watkinson, M. Motevalli and J. F. Lesin, *Dalton Trans.*, 2010, **39**, 53.
8 C. G. Pierpont and C. W. Lange, *Prog. Inorg. Chem.*, 1994, **41**, 331.
9 T. S. Sheriff, P. Carr and B. Piggott, *Inorg. Chim. Acta*, 2003, **348**, 115.
10 A. Panja, N. Ch, M. Patra, P. Brandão, C. E. Moore, D. M. Eichhorn and A. Frontera, *J Mol. Catal. A-Chem.*, 2016, **412**, 56.
11 A. Panja, N. C. Jana and P. Brandão, *J. Inorg. Biochem.*, 2016, **159**, 96.
12 R. Willstatter and F. Muller, *Ber. Dt. Chem. Ges*, 1911, **44**, 2184.
13 F. D. Snell and C. T. Snell, in *Colorimetric Methods of Analysis,* vol. 2A, 3rd ed, D. Van Nostrand Company, Princeton, NJ, 1959, pp. 306-308.
14 SAINT V8.34A, Bruker AXS Inc., 2013.
15 SADABS V2014/5, Bruker AXS Inc., 2014.
16 SHELXS-2014/7, Sheldrick, 2014.
17 SHELXL-2014/7, Sheldrick, 2014.
18 SHELXTL, Bruker AXS Inc., 2014.
19 F. Zetzsche and S. Sukiennik, *Helvetica Chimica Acta*, 1927, **10**, 91.
20 G. F. Koser, *J. Org. Chem.*, 1977, **42**, 1474.
21 H. Boettcher, H. G. O. Becker, V. L. Inanov and M. G. Kusmin, *Chimia*, 1973, **27**, 437.
22 SciFinder, https://www.cas.org/products/scifinder, (accessed 20th October 2017). The pKa gives a measure of the position of the equilibrium and the stability of the conjugate base for a parent acid but perhaps does not give a direct indication of the ease of removal of the proton.
23 S. R. Cooper, J. R. Hartman and B. M. Foxman, *Inorg. Chem.*, 1984, **23**, 1381.
24 C. J. Rolle III, K. I. Hardcastle and J. D. Soper, *Inorg. Chem.,* 2008, **47**, 1892.

View Article Online
DOI: 10.1039/C7NJ02725G



# Nucleophile and Base Differentiation of Pyridine in Reaction with Tetrahalocatechols and the Formation of Manganese(III)-Catecholate and Pyridinium-Catecholate Complexes for the *in situ* Generation of Hydrogen Peroxide from Dioxygen

Nicholas Bakewell[a], Rumintha Thavarajah[b], Majid Motevalli[c] and Tippu S. Sheriff*[c]

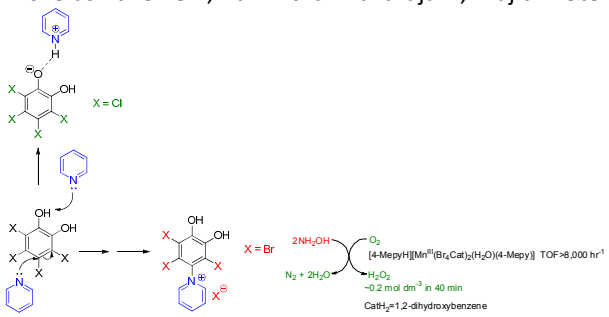


The structures of two novel pyridinium catecholates are reported by reaction of pyridine with tetrachloro-*o*-benzoquinone and tetrabromocatechol; with tetrachlorocatechol pyridine acts as a base with the structure of the pyridinium-catecholate salt reported.